



HAL
open science

Different glycoforms of prostate-specific membrane antigen are intracellularly transported through their association with distinct detergent-resistant membranes

Deborah Castelletti, Marwan Alfalah, Martin Heine, Zeynep Isguder, Ruth Schmitte, Giulio Fracasso, Marco Colombatti, Hassan Y. Naim

► To cite this version:

Deborah Castelletti, Marwan Alfalah, Martin Heine, Zeynep Isguder, Ruth Schmitte, et al.. Different glycoforms of prostate-specific membrane antigen are intracellularly transported through their association with distinct detergent-resistant membranes. *Biochemical Journal*, 2007, 409 (1), pp.149-157. 10.1042/BJ20070396 . hal-00478777

HAL Id: hal-00478777

<https://hal.science/hal-00478777>

Submitted on 30 Apr 2010

HAL is a multi-disciplinary open access archive for the deposit and dissemination of scientific research documents, whether they are published or not. The documents may come from teaching and research institutions in France or abroad, or from public or private research centers.

L'archive ouverte pluridisciplinaire **HAL**, est destinée au dépôt et à la diffusion de documents scientifiques de niveau recherche, publiés ou non, émanant des établissements d'enseignement et de recherche français ou étrangers, des laboratoires publics ou privés.

**Different Glycoforms of Prostate-Specific Membrane Antigen
are intracellularly transported through their Association
with Distinct Detergent-Resistant Membranes**

Deborah Castelletti[‡]ϕ, Marwan Alfalah[‡]ϕ, Martin Heine[‡]ϕ, Zeynep Isguder[‡], Ruth Schmitte[‡],
Giulio Fracasso[§], Marco Colombatti[§], and Hassan Y. Naim[‡]*

[‡]Department of Physiological Chemistry, University of Veterinary Medicine Hannover, Hannover, Germany, and [§]Department of Pathology, University of Verona, Italy

*Corresponding author: Hassan Y. Naim, Ph.D., Department of Physiological Chemistry, University of Veterinary Medicine Hannover, Bünteweg 17, D-30559 Hannover, Germany, Tel: +49 511 953 8780, Fax: +49 511 953 8585, E-mail: hassan.naim@tiho-hannover.de

ϕ Authors contributed equally to this paper

Abstract

Hormone-refractory prostate carcinomas as well as the neovasculature of different tumours express high levels of prostate-specific membrane antigen (PSMA). PSMA is a type II-transmembrane glycoprotein and a potential tumour marker for both diagnosis and passive immunotherapy. Here, we report on the association of PSMA with detergent-resistant membranes (DRMs) at different stages of the protein maturation pathway in LNCaP cells. At least three PSMA glycoforms were biochemically identified based on their extractability behaviour in different non-ionic detergents. In particular, one precursor glycoform of PSMA is associated with Tween 20-insoluble DRMs, whereas the complex glycosylated protein segregates into membrane structures that are insoluble in Lubrol WX and display a different lipid composition. Association of PSMA with these membranes occurs in the Golgi compartment together with the acquisition of a native conformation. PSMA homodimers reach the plasma membrane of LNCaP cells in Lubrol WX-insoluble lipid/protein complexes. At the steady state the majority of PSMA remains within these membrane microdomains at the cell surface. We conclude that the intracellular transport of PSMA occurs through populations of DRMs distinct for each biosynthetic form and cellular compartment.

Running Title: Interaction of PSMA with DRMs

Abbreviations: Prostate-specific membrane antigen, PSMA; endo- β -acetylglucosaminidase, endo H; endoplasmic reticulum, ER; Triton-X 100, TX-100; phosphate buffered saline, PBS; detergent-resistant membranes, DRMs; Dipeptidylpeptidase IV, DPPIV.

Introduction

The prostate specific membrane antigen (PSMA) (1) was initially immunisolated from a lymph node metastasis of a prostate carcinoma (2). Increased expression of PSMA in prostate cancer cells with respect to healthy tissues (3) and its *de novo* synthesis in the neovasculature of many solid tumors (4) render PSMA an attractive marker for prostate tumor diagnosis (5) as well as targeted immunotherapy. In particular, PSMA represents a very suitable target for antibody-vehicled drugs or immunotoxins (6) due to high levels of the protein at the cell surface and efficient antibody-mediated internalization (7).

PSMA is a type II transmembrane glycoprotein of about 100 kDa (8) that is transported to the apical membrane in polarized epithelial cells (9). Its high level of N-glycosylation, to which 25 % of the molecular weight can be ascribed, dictates the correct folding and function that are directly associated with the homodimeric quaternary structure (10). A striking feature in the biosynthetic pathway of PSMA is its trafficking between the endoplasmic reticulum (ER) and the Golgi apparatus and the unusual properties with respect to acquisition of native conformation and intracellular transport (11). In fact, PSMA exits the ER in an unfolded state at a slow rate and acquires resistance to proteolytic cleavage only after it has reached the *medial-/trans*-Golgi. Importantly, PSMA does not require complete processing of N- or O-glycans in the Golgi in order to be transported to the cell surface. While several features of the maturation and trafficking pathways of PSMA are resolved meanwhile, the association of PSMA with the membrane at various stages of its secretory pathway is unknown. These aspects are of primordial importance in the cell physiology of PSMA and towards the assessment of the molecular mechanisms that regulate its expression in prostate cancer.

In this paper we examined the association of PSMA with specialized membranes along the secretory pathway, making use of its extraction properties with a variety of detergents. This is based on the fact that the major constituents of biological membranes - lipids and proteins - determine together the heterogeneous composition of different cell compartments (12) and presumably also of subdomains within the same membrane (13). It is therefore likely that PSMA would associate with different types of membranes throughout its life cycle, which may regulate its presence in a particular cellular compartment and govern its intracellular transport kinetics. Current concepts have designated these specialized microdomains as 'lipid rafts' (14) in virtue of their ability to form a 'liquid-ordered'

phase that is dispersed into a 'liquid-disordered' phase of the lipid bilayer. These microdomains can be biochemically isolated as detergent-resistant membranes (DRMs) upon solubilization with non-ionic detergents such as Triton X-100 (15) and represent tightly packed membrane structures that are enriched in sphingolipids and cholesterol (16). The biological relevance of DRMs has been demonstrated in numerous cellular events, such as signal transduction pathways (17), cell entry of viral particles (18), and membrane trafficking (19). Along these concepts, association of membrane proteins with lipid microdomains occurs on the cell surface as well as in intracellular compartments. Several lines of evidence have unequivocally demonstrated that many apical proteins are recruited to TX-100-insoluble DRMs in the *trans*-Golgi network prior to their delivery to the apical membrane (20). The association of membrane proteins with lipid microdomains or DRMs occurs through the transmembrane domains or glycosylphosphatidylinositol anchors (21) and may implicate accessory proteins that function as receptors for N- or O-glycans that act as sorting signal (22-25).

Recently, mild detergents other than TX-100 have also been utilized in the characterization of membrane microdomains with different lipid and protein compositions (26). Many membrane proteins that are entirely soluble in TX-100 reveal insoluble characteristics with detergents such as Lubrol, Tween 20 or Brij 98 (13, 27, 28). Interestingly, the extraction behaviour of the mannose-rich ER-located precursor forms of several apical and basolateral proteins with Tween 20 pointed to the existence of an early pre-Golgi sorting mechanism (29). It is obvious therefore that the heterogeneity of DRMs depends not only on selective enrichment in some lipids and proteins (26), but also on specific intracellular localization and function.

In this paper we show that PSMA in LNCaP cells (2) associates with two different types of membrane microdomains. The specific biosynthetic forms of PSMA from distinct intracellular compartments are recruited into lipid microdomains of different composition, implicating thus compartment-specific DRMs in intracellular trafficking.

Materials and methods

Materials

Tissue culture material was purchased from Greiner (Hamburg, Germany). RPMI-1640 medium, methionine-free modified Eagle's medium (MEM), and supplemental reagents (penicillin, streptomycin, and glutamine) were from PAA Laboratories GmbH (Pasching, Austria). Fetal calf serum, folic acid, trypsin and the proteinase inhibitors pepstatin, leupeptin, aprotinin, and trypsin-chymotrypsin inhibitor were from Sigma Chemical Co. (Deisenhofen, Germany), whereas phenylmethylsulfonyl fluoride, antipain, and soybean trypsin inhibitor were from Roche Diagnostics (Mannheim). Poly-D-Lysine used to coat tissue culture dishes, TX-100, and the specific inhibitors of N-glycosylation deoxymannojirimycin (dMM) and deoxynojirimycin (dNM) were also obtained from Sigma Chemical Co. L-[³⁵S]-methionine (>1000 Ci/mmol) and protein A-sepharose was from Amersham Biosciences Inc. (Freiburg, Germany). Acrylamide, N,N'-methylenebisacrylamide, TEMED, and Tween 20 were purchased from Carl Roth GmbH (Karlsruhe, Germany). SDS, ammonium persulfate, and dithiothreitol were obtained from Merck, (Darmstadt, Germany). Endo- β -acetylglucosaminidase H (endo H) was from New England BioLabs (Frankfurt, Germany), Brij 58 P from Fluka (Steinheim, Germany) and Lubrol WX from MP Biomedicals (Eschwege, Germany). For biotinylation experiments and western blotting, sulfosuccinimidobiotin (EZ-Link Sulfo-NHS-Biotin) from Pierce (Rockford, IL, USA) was used; streptavidin horseradish peroxidase and streptavidin agarose were from Sigma Chemical Co. (Deisenhofen, Germany), whereas the Hybond-P PVDF membranes and the ECL plus Western Blotting Detection System were both purchased from Amersham Bioscience Inc. (Freiburg, Germany).

Antibodies

Two anti-PSMA monoclonal antibodies (mAb) were used. The 7E11 mAb (2) binds the cytosolic tail of the protein, whereas the J591 mAb (7) recognizes an extracellular epitope of PSMA. Dipeptidylpeptidase IV (DPPIV) from the human colon carcinoma cell line Caco-2 (30) was detected in western blots by the mAb HBB 3/153 (31). Commercial mAb against flotillin-2 and rho A were from Santa Cruz Biotechnology (Heidelberg, Germany), whereas the calnexin-specific mAb was from Becton Dickinson (Heidelberg, Germany). Anti-mouse peroxidase-conjugated secondary antibodies used in western blotting were from Amersham Bioscience Inc. (Freiburg, Germany).

Immunoprecipitation

PSMA was immunoprecipitated from total lysates of LNCaP cells (2), grown at 60 to 70 % confluence in 10 cm Petri dishes in RPMI medium supplemented with folic acid (40 mg/l) and 10 % fetal calf serum. Cells were biosynthetically labelled with 100 μ Ci L-[³⁵S]-methionine for different time intervals, washed twice with ice-cold phosphate buffered saline (PBS) and solubilized for 1 h at 4 °C in the presence of 1 % TX-100/PBS and a mixture of proteinase inhibitors (1 mM phenylmethylsulfonyl fluoride, 1 μ g/ml pepstatin, 5 μ g/ml leupeptin, 5 μ g/ml aprotinin, 1 μ g/ml antipain and 50 μ g/ml trypsin-chymotrypsin inhibitor). After removal of cell debris by centrifugation, PSMA was immunoprecipitated by using a combination of the 7E11 (2) and J591 (7) mAbs for 1 h at 4 °C. Antigen-antibody complexes were then recovered with protein A-sepharose, denatured, and loaded on 6 % polyacrylamide gels under reducing conditions (32). Proteins were finally detected by autoradiography (using a Phosphor Imager from Bio-Rad) upon exposure to Kodak X-Omat AR films.

In order to obtain an accumulation of newly synthesized proteins in the early compartments, cells were first pulse labelled for 30 min at 37 °C and then incubated for further 5 h either at 15 °C, at 20 °C, or at 37 °C. Sensitivity of PSMA to trypsin digestion was assayed by incubating immunoprecipitated proteins with 5 μ g trypsin for 30 min, according to the protocol described previously (11). In some assays, the sensitivity of PSMA to endo H was also tested after immunoprecipitation (33).

DRM extraction

LNCaP cells that reached 60-70 % confluence were labelled with [³⁵S]-methionine for the time intervals specified in each experiment. After washing twice with ice-cold PBS, cells were solubilized in PBS containing 1 % (w/v) detergent and a cocktail of proteinase inhibitors. Lubrol WX, Tween 20, Brij 58 P, and TX-100 were used. Cells were first homogenized with a 21 G needle and then maintained on ice for 1-3 h, depending on the experiment. Afterwards, samples were centrifuged at low-speed (15 min at 2000 g) and cell debris was discarded before a centrifugation at 100,000 g was performed for 90 min. The supernatant (S) and pellet (P) obtained, corresponding to the soluble and the insoluble fractions, respectively, were separately analysed for presence of PSMA. Prior to immunoprecipitation, the pellet fractions (P) were solubilized either under native or under denaturing conditions. In order to maintain a native conformation of the proteins, pellets were resuspended in 1 ml 1 % TX-100/PBS for 1 h. Alternatively, they were first dissolved in 100 μ l 1 % SDS/PBS, boiled 5 min at 95 °C and then diluted with 900 μ l 1 % TX-100/PBS. After 30 min on

ice, the non-solubilized material was removed by centrifugation and the supernatants were further processed. PSMA from both fractions (S, P) was immunoprecipitated by a combination of the 7E11 and J591 mAbs, which recognize both native and denatured PSMA (11). When association with lipid microdomains was studied in relation to glycosylation properties of PSMA, cells were incubated, prior and during labelling, with specific inhibitors of the N-glycans processing, i.e. dNM and dMM, used both at 5 mM.

Additionally, in other experiments association of PSMA with DRMs was investigated by a discontinuous sucrose-density gradient, modifying a protocol reported previously (34). For this, LNCaP cells were lysed with 0,5 % (w/v) of the indicated detergent in PBS (TX-100, Lubrol WX, and Tween 20), according to the methodology described above. After the low-speed centrifugation step, the sample was diluted to a final sucrose-concentration of 40 % and laid onto a 80 % sucrose-cushion. The 1 ml sample was then overlaid with 7 ml of 30 % sucrose and 1 ml of 5 % sucrose on the top, and finally centrifuged for 18 h at 100,000 g with a swing-out rotor. Nine fractions of 1 ml each were collected from the top and analysed for the protein content by western blotting. The distribution of the marker proteins flotillin-2 and rho A in LNCaP cells was tested as positive and negative control, respectively. Confluent Caco-2 cells were used in order to analyse the distribution of human DPPIV and calnexin in similar gradients after solubilization with 0.5 % TX-100.

Lipid analysis

Total lysates of LNCaP cells were prepared as described in the previous paragraph by using 1 % of TX-100, Lubrol WX, and Tween 20, all dissolved in PBS. Pellets obtained after 90 min of centrifugation at 100,000 g were washed twice with chilled PBS (at each step samples were centrifuged for 10 min at 15,000 g). Phospholipids, sphingolipids and cholesterol were extracted from the pellets by following the method of Bligh and Dyer (35). The content in different classes of phospholipids was further analysed according to Meyer et al. (36). Results were represented as mean values and standard deviation, based on four independent experiments.

DRMs at the cell surface

Cell surface proteins in LNCaP cells were biotinylated according to the protocol described in ref. 11. Following solubilization with 1 % Lubrol WX/PBS, the samples were centrifuged at 100,000 g to recover the Lubrol WX-insoluble membranes, as described above. In a control experiment, biotinylated cells were lysed with 1 % TX-100/PBS instead. PSMA was immunisolated from the total lysate, as well as from the S and P fractions, and equally split into

two parts to be analysed by SDS-PAGE and western blotting. The use of streptavidin allowed the selective detection of PSMA on the cell surface, whereas PSMA-specific antibodies visualized the total amount of PSMA as comparison. As a supplemental control, biotinylated proteins were precipitated first using streptavidin agarose beads and analysed by a western blot using PSMA antibodies instead.

PSMA was also immunoprecipitated from the cell surface of radiolabelled LNCaP cells by using the J591 mAb, dissolved in 3 ml of chilled RPMI medium (11). After 45 min on ice in the presence of the anti-PSMA antibody, the cells were solubilized for 1 h with 1 % Lubrol WX/PBS as well as lysate from unlabelled LNCaP cells as source of competing PSMA molecules for the unbound antibodies. The soluble and insoluble materials were separated by ultracentrifugation (see above) and PSMA was recovered by addition of protein A-sepharose. The pellet fractions were resuspended in 1 % TX-100/PBS to preserve the antigen-antibody interactions. In addition, intracellular PSMA from both soluble and insoluble fractions was immunoprecipitated with the combination of mAbs 7E11 and J591. Proteins were finally separated by 6 % SDS-PAGE and analysed by autoradiography.

Analysis of the quaternary structure

Monomers and dimers of PSMA molecules from LNCaP cells were separated by sucrose-density gradients under native conditions and then immunoisolated. Cells were pulse labelled for different time intervals with 100 μ Ci L-[³⁵S]-methionine, washed and lysed for 2 h with 6 mM dodecyl- β -maltoside, dissolved in 100 mM NaCl and 50 mM Tris-HCl pH 7.5 (37). After a centrifugation step at 10,000 g to remove cell debris, cell lysates were loaded on the top of 5-25 % (w/v) continuous sucrose gradients that were centrifuged at 100,000 g for 18 h (4 °C). Fractions of 500 μ l each were collected and immunoprecipitated for the detection of PSMA (see above). As a control, distribution of human DPPIV was also investigated, by performing a gradient under the same conditions, from a lysate of Caco-2 cells pulse labelled for 30 min.

Results

Biosynthesis of PSMA in LNCaP cells

PSMA is endogenously overexpressed in LNCaP cells, a cell line derived from a human prostate adenocarcinoma which had metastasized to the lymph nodes (1). One initial aim of this study was to determine the biosynthetic features and intracellular transport of newly synthesized PSMA molecules in this cellular model. PSMA was immunisolated by using a combination of two mAbs, recognizing the luminal tail of the protein (mAb J591) and an intracellular epitope downstream the transmembrane domain (mAb 7E11). The two main biosynthetic forms of PSMA in LNCaP cells are the mannose-rich form (PSMA_M) and the complex glycosylated form (PSMA_C) as assessed by their reactivity towards endo H (33) (Fig. 1A). The complex glycosylated form of PSMA in LNCaP cells is only slightly larger than the mannose-rich form and differs in this respect markedly from that generated in transfected COS-1 cells (11) pointing thus to variations in the extent of glycan processing in the Golgi compartment of these two cell types. Nevertheless, the conversion rate of the precursor protein into the complex PSMA is conserved (data not shown). The acquisition of PSMA to a protease-resistant correct conformation occurs in LNCaP cells at a later stage of biosynthesis. In fact, the ER-resident form PSMA_M was completely sensitive to trypsin, whereas the protein became trypsin-resistant after acquisition of complex glycosylation (Fig. 1B). These findings were corroborated in a series of temperature block experiments combined with protease treatments. LNCaP cells were metabolically labelled at 37 °C and subsequently chased at 15 °C revealed exclusively the mannose-rich form of PSMA due to the transport block of the protein in the early secretory pathway. This form was completely sensitive to trypsin. At 20 °C PSMA reaches the Golgi and is blocked there. Processing of PSMA at this temperature to a complex form is not efficient and the majority of the protein is retained in its mannose-rich glycosylated form that maintained a trypsin-sensitive conformation. Further incubation of the cells at 37 °C allowed formation of mature PSMA that acquires trypsin-resistance and has presumably acquired a folded structure. Similarly, when cells were labelled continuously at 37 °C, only the mature form obtained was trypsin-resistant. These data are comparable with previous findings in another cellular system (11) and unequivocally indicate that regardless of the cellular system the process of folding of PSMA extends from the ER to the Golgi, the site of complex glycosylation, and represents therefore a unique property of the PSMA protein.

Association of PSMA with DRMs of different composition

Many transmembrane proteins associate with lipid components in the membrane bilayer, forming structural and functional platforms or microdomains. These platforms can play a crucial role in fundamental cellular events, including intracellular trafficking and protein sorting in polarized epithelial cells (20, 23). Experimentally, membrane microdomains can be isolated based on their insolubility in non-ionic detergents (15). Upon solubilization of cellular extracts with a detergent under controlled conditions, the detergent-resistant membranes can be recovered by either sedimentation or in the floating fractions of sucrose-density gradients. We first set out to investigate whether PSMA associates with sphingolipid/cholesterol-enriched TX-100-insoluble DRMs, which have been initially characterized to be implicated in protein transport and sorting (21). In a first set of experiments we analysed the solubility properties of PSMA in LNCaP cells that were labelled for 5 h with [³⁵S]-methionine, during which time the mannose-rich and complex glycosylated biosynthetic forms could be identified. Fig. 2A shows that both PSMA_M and PSMA_C were completely extractable with 1 % TX-100. Recent observations have demonstrated the existence of novel types of DRMs with structures that differ in their lipid composition from the TX-100 DRMs and contain proteins that are usually entirely soluble in TX-100 (29). These DRMs can be extracted with several non-ionic detergents, such as Lubrol WX, Tween 20 and Brij 58. We asked therefore whether (i) DRMs containing PSMA do exist and (ii) if these DRMs could discriminate between the major two biosynthetic forms of PSMA. As shown in Fig. 2B, PSMA was found partially insoluble in Lubrol WX, Tween 20 and Brij 58. More importantly, PSMA_C and PSMA_M are differentially partitioned into the soluble and insoluble DRM-containing fractions. In particular, the majority of PSMA molecules insoluble in Tween 20 were of the mannose-rich form. Relative amounts of PSMA_C and PSMA_M in each fraction are graphically represented in Fig. 2C. The two other detergents, Lubrol WX and Brij 58, solubilized PSMA in a comparable manner as assessed by the similar patterns of protein distribution (Fig. 2C). In fact, after 5 h of labelling the ratio of PSMA_C in the insoluble pellet fraction of both detergents amounted to three times as much as in the Tween 20 pellets, whereas the soluble fraction mostly contained the mannose-rich form.

The detergent extractability of PSMA was evaluated also by sucrose-density centrifugation, based on the ability of DRM structures to float and be recovered on the top of sucrose gradients (34). Due to the similar distribution profile of PSMA in the presence of Lubrol WX and Brij 58, we focused only on one of them, Lubrol WX, and compared the extraction profiles with those of Tween 20. As shown in Fig. 3A, PSMA was not detected in the floating fractions of the discontinuous sucrose gradient when TX-100 was utilized. As a control of a membrane glycoprotein that is associated with TX-100-specific DRMs we considered the intestinal DPPIV expressed in Caco-2

cells (Fig. 3B). DPPIV was recovered in the floating fractions upon solubilization with TX-100 confirming previous data on the association of this protein with TX-100-insoluble DRMs (24). In the same gradient we examined the distribution of calnexin, a membrane-bound chaperone of the ER, and showed that this protein was not retained in the DRM fractions (38). These results together demonstrate unequivocally that PSMA is not associated with TX-100-insoluble DRMs. Furthermore we analysed the distribution of PSMA in sucrose gradients of cellular extracts obtained with Tween 20 and Lubrol WX. As shown in Fig. 3A, the upper fractions of the sucrose-gradients contained PSMA when Tween 20 and Lubrol WX were used, thus supporting the results obtained in the ultracentrifugation experiments (Fig. 2). As positive and negative controls for all three detergents, we used two protein markers that are DRM-associated and non-associated, respectively. As shown in Fig. 3C, flotillin-2 was recovered in the DRM floating fractions, while rho A was retained in the bottom fractions of the gradients, thus supporting the finding that PSMA is associated with Tween 20- and Lubrol WX-DRMs.

Lipid composition of membranes isolated with different detergents

In view of the differential association of PSMA with DRMs corresponding to cellular extraction with Lubrol WX and Tween 20 but not TX-100, we performed a comparative analysis of the lipid contents of the DRMs. Fig. 4A shows a substantial decrease in the contents of sphingolipids (SL) and cholesterol (Chol) upon solubilization with Lubrol WX and Tween 20 as compared to TX-100, which DRMs are enriched in sphingolipids and cholesterol (21). The relative proportions of different classes of phospholipids (PL) have been resolved by HPLC and are depicted in Fig. 4B. The most remarkable difference is the proportion of phosphatidylethanolamine (PE), which is increased about 6- and 8-fold in the DRMs of Tween 20 and Lubrol WX, respectively. Quantitative differences emerged also by comparing membranes isolated with Lubrol WX and Tween 20. In particular, the proportion of phosphatidylinositol (PI), phosphatidylserine (PS) and phosphatidylcholine (PC) differed significantly, suggestive of specific physicochemical properties discriminating the two distinct types of DRMs.

Association with DRMs during biogenesis of PSMA

The differential association of the biosynthetic forms of PSMA, i.e. PSMA_M and PSMA_C, with Tween 20- and Lubrol WX-DRMs (Fig. 2), as well as the differences in the lipid composition of these DRMs, raised the question of a possible crucial role of these entities as platforms that dictate the various phases of the trafficking of PSMA. To this end, LNCaP cells were subjected to pulse-

chase and lysed with either Tween 20 (Fig. 5A-B) or Lubrol WX (Fig. 5C). DRMs were then isolated by sedimentation, followed by immunoisolation of PSMA. After 30 min of pulse, the protein was still completely in its mannose-rich form, coming along with an ER localization. Interestingly, the use of Tween 20 allowed the discrimination between two distinct forms of PSMA (Fig. 5A). Apparently, these two forms display very close molecular weights that were too difficult to resolve when the protein was isolated from total cell lysates (Fig. 1). Based on their sensitivity to endo H and the shift in the size to similar protein forms (Fig. 5B), we were able to confirm that both protein bands are core-glycosylated ER-resident forms. The higher band, PSMA_{M1}, was recovered exclusively from the DRM or pellet (P) fraction and persists up to at least 90 min of chase, indicative of a very slow conversion and further processing. On the contrary, the Tween 20-soluble form, PSMA_{M2}, is converted faster into the complex glycosylated protein, which is in turn also soluble in Tween 20. This clearly indicates that the localization of Tween 20-insoluble DRMs containing PSMA is along the early secretory pathway. The use of Lubrol WX gave a completely different pattern (Fig. 5C). Both ER-forms of PSMA are almost completely soluble, whereas the complex glycosylated form appears as a very faint band at the 30 min-chase point also in the soluble fraction. Subsequently, PSMA_C starts to be isolated in association with Lubrol WX-insoluble DRMs as well (60 min chase). Recovery of PSMA_C in the DRM or P fraction increases and reaches a maximum after 120 min into the chase.

In view of the association of one glycoform of PSMA with Tween 20-DRMs, we determined whether this association at early stages of the secretory pathway depends on the glycosylation state of the protein. To this end, the glycoforms were modulated by using dNM, an inhibitor of the ER-located glucosidase I that is responsible for the initial trimming of the terminal glucose of the core glycan chain in the ER (39). Treatment of LNCaP cells with dNM during a labelling period of 30 min resulted in the detection of a slightly higher band that was recovered in the DRM and also in the soluble fraction upon solubilization with Tween 20 (Fig. 6A). It is likely therefore that the subcellular localization rather than the glycan moiety determines the association of PSMA with DRMs. To substantiate these data, we examined the influence of modification of the sugar chains in the Golgi compartment on the association of PSMA with Lubrol WX-DRMs. For this we utilized dMM, a modulator of complex glycosylation through inhibition of Golgi mannosidase I (39). As shown in Fig. 6B, PSMA generated in the presence of dMM reveals an apparent molecular weight approximately similar to that of the mannose-rich polypeptide and is also endo H-sensitive (data not shown). Despite this, this form is associated with Lubrol WX-DRMs as its complex glycosylated

PSMA_C counterpart obtained in the absence of dMM. In conclusion, the subcellular location of PSMA dictates its association with Tween 20- or Lubrol WX-DRMs.

Cell surface PSMA is almost entirely associated with Lubrol-insoluble DRMs

The J591 mAb was used to selectively immunoprecipitate PSMA molecules at the cell surface (Fig. 7A). After formation of antigen-antibody complexes at 4 °C, the cells were lysed with either TX-100 for the total lysate or Lubrol WX for isolation of the DRMs. PSMA present at the plasma membrane (PM) was compared with its counterpart that is located intracellularly (I) in both the soluble (S) and the insoluble DRM (P) fractions. During 5 h of continuous pulse labelling about 15 % of PSMA was detected at the cell surface, thus confirming the relatively slow transport rate of newly synthesized PSMA_C molecules (11). Interestingly, PSMA located at cell surface is nearly completely associated with Lubrol WX-insoluble microdomains. The biosynthetic data were corroborated by another approach (Fig. 7B). Here, LNCaP cells were biotinylated and PSMA was first immunoprecipitated and then analysed by western blotting. Detection using streptavidin (left panel) or anti-PSMA antibodies (right panel) allowed discrimination between PSMA_C at the plasma membrane and total PSMA, respectively. The data reveal that a major part of PSMA_C is distributed at the plasma membrane of LNCaP cells at steady-state and most of it was found associated with Lubrol WX-associated DRMs. The ratio between the individual fractions was also confirmed by the converse approach: here, the biotinylated proteins were precipitated first and then subjected to a western blot using anti-PSMA antibodies (Fig. 7C).

PSMA forms homodimers temporally close to acquiring complex glycosylation

It has been reported that native PSMA is expressed in homodimeric forms that constitute the enzymatically-active form of PSMA (10). However, the cellular localization of the dimerization event had not been assessed yet. For this purpose we analysed the quaternary structure of PSMA utilizing continuous sucrose density gradients (5-25 %). To track the conversion of a particular form of PSMA to another along the secretory pathway, the cells were subjected to a pulse-chase protocol (Fig. 8). After 15 min of pulse labelling, PSMA occurs in two mannose-rich glycosylated forms that have been previously discriminated based on their solubility or insolubility behaviour in the Tween 20 detergent (Fig. 5A-B). Both of these forms are in a monomeric state, since they were retained in fractions corresponding to a single peak that coincides with that of the control protein DPPIV. The mannose-rich form of DPPIV has an almost similar size to that of PSMA and has been shown to dimerize only after complex glycosylation in the Golgi (40). Dimerization of complex glycosylated

DPPIV is confirmed in Fig. 8 (last panel, fractions 13-16). When LNCaP cells were labelled for 45 min, three distinct protein forms could be detected. The two precursor forms nearly co-migrate peaking at fraction 8 whereas complex glycosylated PSMA is distributed in the following fractions with a maximum into fractions 12-13. After 4 h of chase, the same population of PSMA molecules was almost completely converted into dimeric PSMA_C. It should be noted that no PSMA_C molecules were detected in the fraction that coincided with the peak of monomer-rich PSMA. Taken together, it can be concluded that dimerization of PSMA and the acquisition of its complex glycosylated form in the Golgi occur temporally close to each other.

Discussion

PSMA is a potential target for prostate cancer treatment (5-7), as well as for solid tumors of different histotype due to its *de novo* expression in the tumor neovasculature (4). Several aspects of its structure, biosynthesis and processing have been elucidated meanwhile, and some of which have revealed surprising findings. In fact, PSMA exits the ER in an unfolded, trypsin-sensitive form and acquires a native correctly folded conformation in the Golgi compartment (11). This folding pattern cannot be ascribed to an impairment of the protein synthesis machinery in heterologous systems (11), since we observed a similar maturation pattern in this study in LNCaP cells, which express the protein endogenously (2). This maturation behaviour does not entirely conform to current concepts of protein folding and quality control mechanisms in the ER. As such PSMA is a unique example of a membrane protein and unravelling of the molecular mechanisms underlying its trafficking and targeting may lead to the identification of novel pathways or modification of established concepts. From a mechanistic point of view it is important to understand the mode of association of PSMA with membranes on its way to the cell surface. This is an essential task by virtue of current knowledge which assigned a role for membrane microdomains as platforms in prostate carcinoma by influencing cancer aggressiveness in the malignant transformation (41, 42). Two distinct caveolin-independent but cholesterol-dependent signalling pathways have been identified in LNCaP cells (43, 44).

Possible interactions of PSMA with membranes in LNCaP cells have not been analysed so far. We therefore set out to investigate the possible association of PSMA with lipid microdomains at different biosynthetic stages. Extraction with distinct detergents allows to isolate DRMs having a different composition (26), which can play a physiological role not only at the cell surface (13) but also in the *trans*-Golgi network and in earlier compartments, where they are involved in cellular trafficking of transmembrane proteins (29). Our data support the existence of functional as well as spatial correlation between trafficking of PSMA and the lipid content of DRMs.

First, PSMA does not associate with TX-100-resistant DRMs that are enriched in cholesterol and sphingolipids (21). Association of transmembrane proteins with this class of membrane microdomains represents a mechanism of apical protein sorting occurring at the level of the *trans*-Golgi network in polarized epithelial cells (20). Although it is localized at the apical membrane (9, 11) and shares striking homologies with the apical protein DPPIV (45) that is associated with cholesterol-/sphingolipids-rich DRMs (24), PSMA is entirely soluble in TX-100. Nevertheless, the extraction properties of PSMA in Tween 20 and Lubrol WX proposed a crucial role of the DRMs in

the trafficking of PSMA. In fact, the two major glycoforms of PSMA reveal distinct extractability profiles with these detergents. Thus, the mannose-rich form associates predominantly with Tween 20-DRMs and the complex glycosylated one is mainly insoluble in Lubrol WX, consistent with the view that PSMA is transported via different membrane microdomains along the secretory pathway. These various DRMs could also be distinguished on the basis of their distinct lipid contents that differ substantially from the composition of TX-100 DRMs. Even though DRM extraction with detergents *per se* is not informative about the spatial localization of membranes, the different biosynthetic forms of PSMA can be considered as a marker for cellular distribution. The selective partitioning of PSMA_M and PSMA_C in distinct DRMs is indicative of an enrichment of Tween 20-DRMs containing PSMA in the ER and of Lubrol WX-DRMs in later compartments.

There is growing evidence supporting diverse modes of association of transmembrane proteins with microdomains along the secretory pathway. Association with Tween 20-insoluble DRMs in the ER, for instance, has been described as early sorting mechanism in polarized cells (29). Protein association with lipid microdomains in the early secretory pathway has been recently reported also for ER-resident proteins (46). Detergents other than TX-100 have been used already to isolate membrane structures from the *trans*-Golgi network as well as from the cell surface. This is the case for the complex glycosylated protein prominin (13), which associates on the cell surface of epithelial cells with DRMs that are soluble in TX-100 but insoluble with Lubrol WX, i.e. in a way similar to PSMA in LNCaP cells. These findings also imply the coexistence of distinct lipid microdomains within the same cell compartment. In fact, whereas several lines of evidence demonstrated the implication of TX-100 DRMs in processes taking place at the plasma membrane (17, 18), the isolation of PSMA-containing DRMs showed the existence of at least one other type of protein/lipid platforms of different composition at the cell surface. Moreover, it is the first time that a switch between membrane structures is described along the maturation pathway of a protein. After interacting with Tween 20-insoluble membranes in the ER, PSMA associates with Lubrol WX-DRMs as soon as it enters the Golgi, where it acquires complex glycosylation. The interaction with Lubrol WX-DRMs is either maintained or renewed once it reaches the plasma membrane. At the steady state, a major part of the PSMA molecules are present at the cell surface and most of them associate with Lubrol WX-DRMs. Since DRMs are dynamic structures in the membranes, the soluble PSMA and the DRM-associated form of the protein are most likely in equilibrium with each other. Whether the existence of Lubrol-DRMs on the cell surface has a physiological function remains to be elucidated.

Our results suggest that the conversion of PSMA into a complex glycosylated protein is a

process spatially related to association with Lubrol WX-insoluble membranes. Also related to association with DRMs is the homodimerization of PSMA, which is achieved temporally close to accomplishing complex glycosylation, which is also taking place in the Golgi. This is supported by the observation that PSMA_C is found as a dimeric protein, whereas the ER-forms are exclusively present as monomers. It has been shown that dimerization of PSMA and acquisition of a functional structure are strictly related to each other (10). While it is clear that dimeric PSMA_C associates with Lubrol WX-insoluble membranes, it is not obvious whether the association with DRMs precedes or follows the dimerization.

In conclusion, the present investigation demonstrates a novel pathway of intracellular protein transport that is dictated by the association of a glycoprotein with distinct membrane microdomains at different stages of its maturation. The identification of DRM-associated PSMA at the plasma membrane of LNCaP cells might be an important step towards unravelling the transition of prostate cells to a neoplastic phenotype and the potential role of these DRMs as signalling platforms at the cell surface. The outcome of these studies is equally important in designing strategies of immunotherapy comprising PSMA-expressing cells.

Acknowledgements

Dr. N.H. Bander (Medical College of Cornell University, New York) is gratefully acknowledged for the gift of the J591 monoclonal antibody. We also thank Dr. E. Sterchi (Institute of Biochemistry and Molecular Biology, University of Berne, Berne, Switzerland) for providing us with the anti-DPPiV (HBB 3/153) monoclonal antibody.

This work was supported by the Deutsche Forschungsgemeinschaft, Bonn, Germany (Grant Na 331/1-4 to H.Y.N.) and MIUR (PRIN 2005) and Fondazione Cassa di Risparmio di Verona, Vicenza, Belluno e Ancona (Bando 2004, "Integrazione tra Tecnologia e Sviluppo di Settore", to M.C.).

Figures Legends

Figure 1. PSMA acquires resistance to trypsin as a complex glycosylated protein

(A) PSMA was immunoprecipitated from total lysates of sub-confluent LNCaP cells that were pulse labelled for 30 or 180 min with [³⁵S]-methionine. Digestion with endo H enzyme allowed discrimination between the complex glycosylated form (PSMA_C, upper bands) and the mannose-rich form (PSMA_M, lower bands). (B) After 30 min labelling at 37 °C, LNCaP cells were maintained for further 5 h at the indicated temperatures (15, 20 or 37 °C). Following lysis and immunoprecipitation with the 7E11 and J591 mAbs, PSMA was treated with 5 µg trypsin (+) or left untreated (-). Proteins were finally subjected to SDS-PAGE on a 6 % acrylamide gel and analysed by autoradiography.

Figure 2. PSMA is completely soluble in TX-100 and partially insoluble in other detergents

(A) After 5 h labelling, LNCaP cells were lysed with 1 % TX-100 for 1 h on ice. Lysates were subjected to 100,000 g for 90 min in order to separate the insoluble and the soluble material. Both fractions were further analysed for the presence of PSMA by immunoprecipitation. Analysis of the total cell lysate is reported as comparison (Tot). (B) The solubility/insolubility properties of PSMA_C and PSMA_M (discriminated based on sensitivity to endo H) were tested in the presence of Lubrol WX, Tween 20 and Brij 58 P, according to the protocol used in (A). (C) The relative proportion of PSMA_C and PSMA_M in each sample was quantified and graphically represented, based on the results of three independent experiments. S, supernatant (soluble fraction); P, pellet (insoluble fraction)

Figure 3. Isolation of DRMs by sucrose-density gradient centrifugation

(A) Lysates of LNCaP cells obtained after solubilization with 0.5 % of either TX-100, Tween 20 or Lubrol WX were subjected to a discontinuous sucrose-density gradient (1ml 5 % - 7 ml 30 %). After centrifugation, one third from each fraction was concentrated and analysed by 6 % SDS-PAGE and western blotting for the presence of PSMA. (B) For TX-100, the distribution profiles of DPPIV and calnexin were considered as positive and negative controls, respectively. To this, Caco-2 cells were used. (C) For all three detergents the distribution of PSMA in LNCaP cells was compared to Flotillin-2 and Rho A, taken as positive and negative controls regarding DRM association. *Lys*, total lysate, prior to fractionation by gradient

Figure 4. Lipid composition of DRMs in LNCaP cells

DRMs were extracted from LNCaP cells by using 1 % TX-100, Lubrol WX or Tween 20 and recovered by sedimentation. (A) The lipid content is presented as relative proportion of either

cholesterol (Chol) or sphingolipids (SL) with respect to total phospholipids (PL). (B) The PL were further resolved by HPLC into the following classes (each reported in percent of total PL): phosphatidylglycerol (PG), phosphatidylethanolamine (PE), phosphatidylinositol (PI), phosphatidylserine (PS), phosphatidylcholine (PC), and sphingomyelin (SM). Results are given as mean and standard deviation based on four independent experiments.

Figure 5. PSMA associates with Tween 20- and Lubrol WX-insoluble DRMs at different stages of protein transport

(A) LNCaP cells were pulsed for 30 min with [³⁵S]-methionine, then washed and further incubated with medium containing an excess of unlabelled methionine for the indicated times. After solubilization with 1 % Tween 20 for 3 h at 4 °C, cell debris and big membrane aggregates were discarded by centrifugation. Supernatants were subjected to 100,000 g centrifugation (90 min) and both the soluble and insoluble fractions obtained were analysed for the presence of PSMA. Isolated proteins were analysed by 6 % SDS-PAGE and detected by autoradiography. (B) Sensitivity of PSMA to endo H digestion after extraction with 1 % Tween 20 from LNCaP cells pulse labelled for 30 min and chased for the respective times. (C) As for panel (A), the same assay and protein analysis was performed. However, Lubrol WX was used instead, in order to isolate DRMs of different composition. S, supernatant (soluble fraction); P, pellet (insoluble fraction)

Figure 6. Association of early forms of PSMA in the presence of glycan-processing inhibitors

LNCaP cells were incubated in methionine-free medium for 2 h and pulsed for 30 min with [³⁵S]-methionine. During both incubation intervals, cells were maintained in the presence of 5 mM dNM (A). Following lysis with 1 % Tween 20, DRM isolation and immunoprecipitation of PSMA were carried out according to the protocol described above. In a similar assay (B), the effect of dMM (5 mM) on PSMA segregation in Lubrol WX-insoluble DRMs was tested. For this experiment, cells were pulse labelled for 3 h. S, supernatant (soluble fraction); P, pellet (insoluble fraction)

Figure 7. PSMA associates with Lubrol WX-insoluble DRMs on the cell surface

(A) PSMA was selectively isolated from the cell surface of LNCaP cells pulse labelled for 5 h. The J591 mAb that recognizes an extra-cellular epitope of the protein was used. Then, cells were lysed 1 h with 1 % Lubrol WX and then subjected to centrifugation at 100,000 g for 1.5 h to obtain a soluble (S) and an insoluble (P) fraction. After recovery of cell surface PSMA (PM) by addition of protein A-sepharose, intracellular PSMA was immunoisolated from the remaining lysate (I). For

comparison, surface-immunoprecipitation was also performed on LNCaP cells lysed by TX-100 for the total amount of PSMA (Total). (B) LNCaP cells were cell surface-biotinylated and lysed with 1 % Lubrol WX. After centrifugation (see above) the insoluble fraction (P) was solubilized with 1 % TX-100 and PSMA was immunoprecipitated from both P and S. Here, the amount of PSMA detected by streptavidin (PM) is compared to the total amount of PSMA in P and S, based on the use of anti-PSMA mAbs in western blotting. (C) As a supplemental control for the amount of surface PSMA found in Lubrol rafts, biotinylated proteins were precipitated using streptavidin beads instead. Western blot analysis of these proteins for the presence of PSMA resulted in a similar ratio as in Fig. 7B. S, supernatant (soluble fraction); P, pellet (insoluble fraction); PM, plasma membrane; I, intracellular fraction; P', supernatant of the streptavidin bead IP of the insoluble fraction; S', supernatant of the streptavidin bead IP of the soluble fraction

Figure 8. PSMA dimerizes temporally close to acquiring its complex glycosylated form

LNCaP cells were pulse labelled for 15 or 45 min (first two panels). Alternatively, they were pulsed for 45 min and then chased for further 4 h to follow the fate of the pulse-labelled PSMA molecules. Cells were solubilized with 6 mM dodecyl- β -maltoside and 1 ml of the lysate was loaded on the top of a 5-25 % continuous sucrose-gradient. After 18 h of centrifugation at 100,000 g, PSMA was immunoprecipitated from each fraction. The distribution of DPPIV was tested under the same conditions, following labelling of Caco-2 cells for 30 min. Reported are the fractions 4 to 16 taken from the twenty 500 μ l-fractions collected in each experiment.

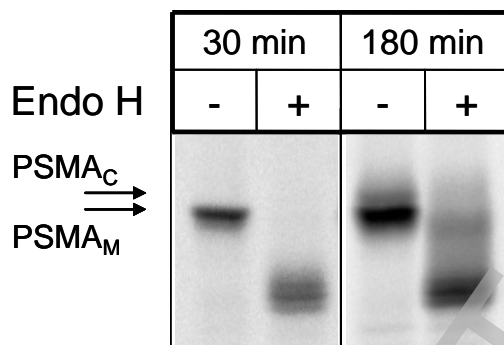
References

- 1 Israeli, R. S., Powell, C. T., Fair, W. R., and Heston, W. D. (1993) Molecular cloning of a complementary DNA encoding a prostate-specific membrane antigen. *Cancer Res.* **53**, 227-230
- 2 Horoszewicz, J. S., Kawinski, E., and Murphy, G. P. (1987) Monoclonal antibodies to a new antigenic marker in epithelial prostatic cells and serum of prostatic cancer patients. *Anticancer Res.* **7**, 927-935
- 3 Israeli, R. S., Powell, C. T., Corr, J. G., Fair, W. R., and Heston, W. D. (1994) Expression of the prostate-specific membrane antigen. *Cancer Res.* **54**, 1807-1811
- 4 Chang, S. S., Reuter, V. E., Heston, W. D., Bander, N. H., Grauer, L. S., and Gaudin, P. B. (1999) Five different anti-prostate-specific membrane antigen (PSMA) antibodies confirm PSMA expression in tumor-associated neovasculature. *Cancer Res.* **59**, 3192-3198
- 5 Landers, K. A., Burger, M. J., Tebay, M. A., Purdie, D. M., Scells, B., Samaratunga, H., Lavin, M. F., and Gardiner, R. A. (2005) Use of multiple biomarkers for a molecular diagnosis of prostate cancer. *Int.J.Cancer* **114**, 950-956
- 6 Jansen, F. K., Blythman, H. E., Carriere, D., Casellas, P., Gros, O., Gros, P., Laurent, J. C., Paolucci, F., Pau, B., Poncelet, P., Richer, G., Vidal, H., and Voisin, G. A. (1982) Immunotoxins: hybrid molecules combining high specificity and potent cytotoxicity. *Immunol.Rev.* **62**, 185-216
- 7 Liu, H., Rajasekaran, A. K., Moy, P., Xia, Y., Kim, S., Navarro, V., Rahmati, R., and Bander, N. H. (1998) Constitutive and antibody-induced internalization of prostate-specific membrane antigen. *Cancer Res.* **58**, 4055-4060
- 8 Barinka, C., Sacha, P., Sklenar, J., Man, P., Bezouska, K., Slusher, B. S., and Konvalinka, J. (2004) Identification of the N-glycosylation sites on glutamate carboxypeptidase II necessary for proteolytic activity. *Protein Sci.* **13**, 1627-1635
- 9 Christiansen, J. J., Rajasekaran, S. A., Moy, P., Butch, A., Goodglick, L., Gu, Z., Reiter, R. E., Bander, N. H., and Rajasekaran, A. K. (2003) Polarity of prostate specific membrane antigen, prostate stem cell antigen, and prostate-specific antigen in prostate tissue and in a cultured epithelial cell line. *Prostate* **55**, 9-19
- 10 Schulke, N., Varlamova, O. A., Donovan, G. P., Ma, D., Gardner, J. P., Morrissey, D. M., Arrigale, R. R., Zhan, C., Chodera, A. J., Surowitz, K. G., Maddon, P. J., Heston, W. D., and Olson, W. C. (2003) The homodimer of prostate-specific membrane antigen is a functional target for cancer therapy. *Proc.Natl.Acad.Sci.U.S.A* **100**, 12590-12595
- 11 Castelletti, D., Fracasso, G., Alfalah, M., Cingarlini, S., Colombatti, M., and Naim, H. Y. (2006) Apical transport and folding of prostate-specific membrane antigen occurs independent of glycan processing. *J.Biol.Chem.* **281**, 3505-3512
- 12 Sprong, H., van der Sluijs, P., and van Meer, G. (2001) How proteins move lipids and lipids move proteins. *Nat.Rev.Mol.Cell Biol.* **2**, 504-513
- 13 Roper, K., Corbeil, D., and Huttner, W. B. (2000) Retention of prominin in microvilli reveals distinct cholesterol-based lipid micro-domains in the apical plasma membrane. *Nat.Cell Biol.* **2**, 582-592
- 14 Simons, K. and Ikonen, E. (1997) Functional rafts in cell membranes. *Nature* **387**, 569-572

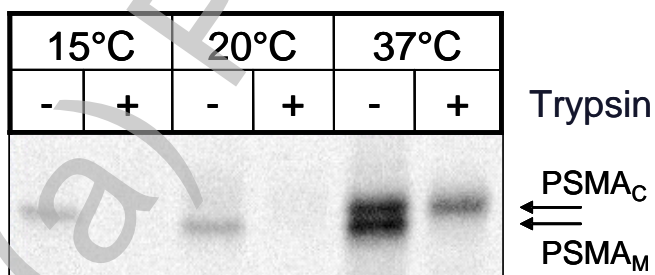
- 15 Schroeder, R. J., Ahmed, S. N., Zhu, Y., London, E., and Brown, D. A. (1998) Cholesterol and sphingolipid enhance the Triton X-100 insolubility of glycosylphosphatidylinositol-anchored proteins by promoting the formation of detergent-insoluble ordered membrane domains. *J.Biol.Chem.* **273**, 1150-1157
- 16 Brown, D. A. and London, E. (2000) Structure and function of sphingolipid- and cholesterol-rich membrane rafts. *J.Biol.Chem.* **275**, 17221-17224
- 17 Simons, K. and Toomre, D. (2000) Lipid rafts and signal transduction. *Nat.Rev.Mol.Cell Biol.* **1**, 31-39
- 18 Chazal, N. and Gerlier, D. (2003) Virus entry, assembly, budding, and membrane rafts. *Microbiol.Mol.Biol.Rev.* **67**, 226-37
- 19 Ikonen, E. (2001) Roles of lipid rafts in membrane transport. *Curr.Opin.Cell Biol.* **13**, 470-477
- 20 Ait, S. T. and Hoekstra, D. (2002) Sphingolipid trafficking and protein sorting in epithelial cells. *FEBS Lett.* **529**, 54-59
- 21 Brown, D. A. and Rose, J. K. (1992) Sorting of GPI-anchored proteins to glycolipid-enriched membrane subdomains during transport to the apical cell surface. *Cell* **68**, 533-544
- 22 Jacob, R., Alfalah, M., Grunberg, J., Obendorf, M., and Naim, H. Y. (2000) Structural determinants required for apical sorting of an intestinal brush-border membrane protein. *J.Biol.Chem.* **275**, 6566-6572
- 23 Alfalah, M., Jacob, R., Preuss, U., Zimmer, K. P., Naim, H., and Naim, H. Y. (1999) O-linked glycans mediate apical sorting of human intestinal sucrase-isomaltase through association with lipid rafts. *Curr.Biol.* **9**, 593-596
- 24 Alfalah, M., Jacob, R., and Naim, H. Y. (2002) Intestinal dipeptidyl peptidase IV is efficiently sorted to the apical membrane through the concerted action of N- and O-glycans as well as association with lipid microdomains. *J.Biol.Chem.* **277**, 10683-10690
- 25 Delacour, D., Cramm-Behrens, C. I., Drobecq, H., Le Bivic, A., Naim, H. Y., and Jacob, R. (2006) Requirement for galectin-3 in apical protein sorting. *Curr.Biol.* **16**, 408-414
- 26 Schuck, S., Honsho, M., Ekroos, K., Shevchenko, A., and Simons, K. (2003) Resistance of cell membranes to different detergents. *Proc.Natl.Acad.Sci.U.S.A* **100**, 5795-5800
- 27 Drevot, P., Langlet, C., Guo, X. J., Bernard, A. M., Colard, O., Chauvin, J. P., Lasserre, R., and He, H. T. (2002) TCR signal initiation machinery is pre-assembled and activated in a subset of membrane rafts. *EMBO J.* **21**, 1899-1908
- 28 Holm, K., Weclawicz, K., Hewson, R., and Suomalainen, M. (2003) Human immunodeficiency virus type 1 assembly and lipid rafts: Pr55(gag) associates with membrane domains that are largely resistant to Brij98 but sensitive to Triton X-100. *J.Virol.* **77**, 4805-4817
- 29 Alfalah, M., Wetzell, G., Fischer, I., Busche, R., Sterchi, E. E., Zimmer, K. P., Sallmann, H. P., and Naim, H. Y. (2005) A novel type of detergent-resistant membranes may contribute to an early protein sorting event in epithelial cells. *J.Biol.Chem.* **280**, 42636-42643
- 30 Rousset, M., Chevalier, G., Rousset, J. P., Dussaulx, E., and Zweibaum, A. (1979) Presence and cell growth-related variations of glycogen in human colorectal adenocarcinoma cell lines in culture. *Cancer Res.* **39**, 531-534
- 31 Hauri, H. P., Sterchi, E. E., Bienz, D., Fransen, J. A., and Marxer, A. (1985) Expression and intracellular transport of microvillus membrane hydrolases in human intestinal epithelial cells. *J.Cell Biol.* **101**, 838-851
- 32 Jacob, R., Weiner, J. R., Stadge, S., and Naim, H. Y. (2000) Additional N-glycosylation and its impact on the folding of intestinal lactase-phlorizin hydrolase. *J.Biol.Chem.* **275**, 10630-10637

- 33 Naim, H. Y., Sterchi, E. E., and Lentze, M. J. (1987) Biosynthesis and maturation of lactase-phlorizin hydrolase in the human small intestinal epithelial cells. *Biochem.J.* **241**, 427-434
- 34 Babiychuk, E. B. and Draeger, A. (2006) Biochemical characterization of detergent-resistant membranes: a systematic approach. *Biochem.J.* **397**, 407-416
- 35 Bligh, E. G. and Dyer, W. J. (1959) A rapid method of total lipid extraction and purification. *Can.J.Biochem.Physiol* **37**, 911-917
- 36 Meyer zu Duttingdorf, H., Sallmann, H., Glockenthor, U., von Engelhardt, W., and Busche, R. (1999) Isolation and lipid composition of apical and basolateral membranes of colonic segments of guinea Pig. *Anal.Biochem.* **269**, 45-53
- 37 Naim, H. Y. and Naim, H. (1996) Dimerization of lactase-phlorizin hydrolase occurs in the endoplasmic reticulum, involves the putative membrane spanning domain and is required for an efficient transport of the enzyme to the cell surface. *Eur.J.Cell Biol.* **70**, 198-208
- 38 Puertollano, R., Martin-Belmonte, F., Millan, J., de Marco, M. C., Albar, J. P., Kremer, L., and Alonso, M. A. (1999) The MAL proteolipid is necessary for normal apical transport and accurate sorting of the influenza virus hemagglutinin in Madin-Darby canine kidney cells. *J.Cell Biol.* **145**, 141-151
- 39 Fuhrmann, U., Bause, E., Legler, G., and Ploegh, H. (1984) Novel mannosidase inhibitor blocking conversion of high mannose to complex oligosaccharides. *Nature* **307**, 755-758
- 40 Jascur, T., Matter, K., and Hauri, H. P. (1991) Oligomerization and intracellular protein transport: dimerization of intestinal dipeptidylpeptidase IV occurs in the Golgi apparatus. *Biochemistry* **30**, 1908-1915
- 41 Freeman, M. R. and Solomon, K. R. (2004) Cholesterol and prostate cancer. *J.Cell Biochem.* **91**, 54-69
- 42 Freeman, M. R., Cinar, B., and Lu, M. L. (2005) Membrane rafts as potential sites of nongenomic hormonal signaling in prostate cancer. *Trends Endocrinol.Metab* **16**, 273-279
- 43 Zhuang, L., Lin, J., Lu, M. L., Solomon, K. R., and Freeman, M. R. (2002) Cholesterol-rich lipid rafts mediate akt-regulated survival in prostate cancer cells. *Cancer Res.* **62**, 2227-2231
- 44 Kim, J., Adam, R. M., Solomon, K. R., and Freeman, M. R. (2004) Involvement of cholesterol-rich lipid rafts in interleukin-6-induced neuroendocrine differentiation of LNCaP prostate cancer cells. *Endocrinology* **145**, 613-619
- 45 Pangalos, M. N., Neefs, J. M., Somers, M., Verhasselt, P., Bekkers, M., van der, H. L., Fraiponts, E., Ashton, D., and Gordon, R. D. (1999) Isolation and expression of novel human glutamate carboxypeptidases with N-acetylated alpha-linked acidic dipeptidase and dipeptidyl peptidase IV activity. *J.Biol.Chem.* **274**, 8470-8483
- 46 Browman, D. T., Resek, M. E., Zajchowski, L. D., and Robbins, S. M. (2006) Erlin-1 and erlin-2 are novel members of the prohibitin family of proteins that define lipid-raft-like domains of the ER *J.Cell Sci.* **119**, 3149-3160

(A)

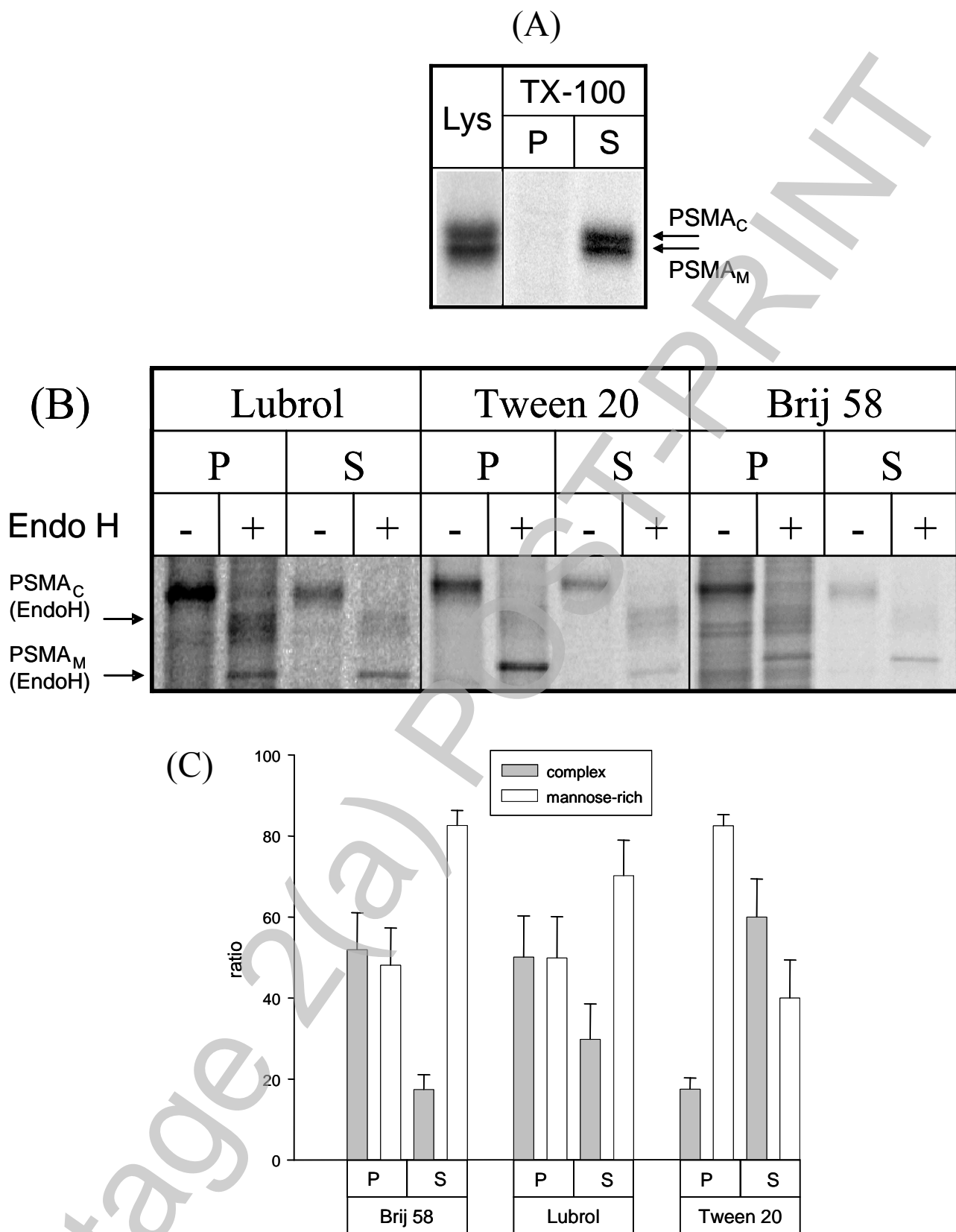


(B)



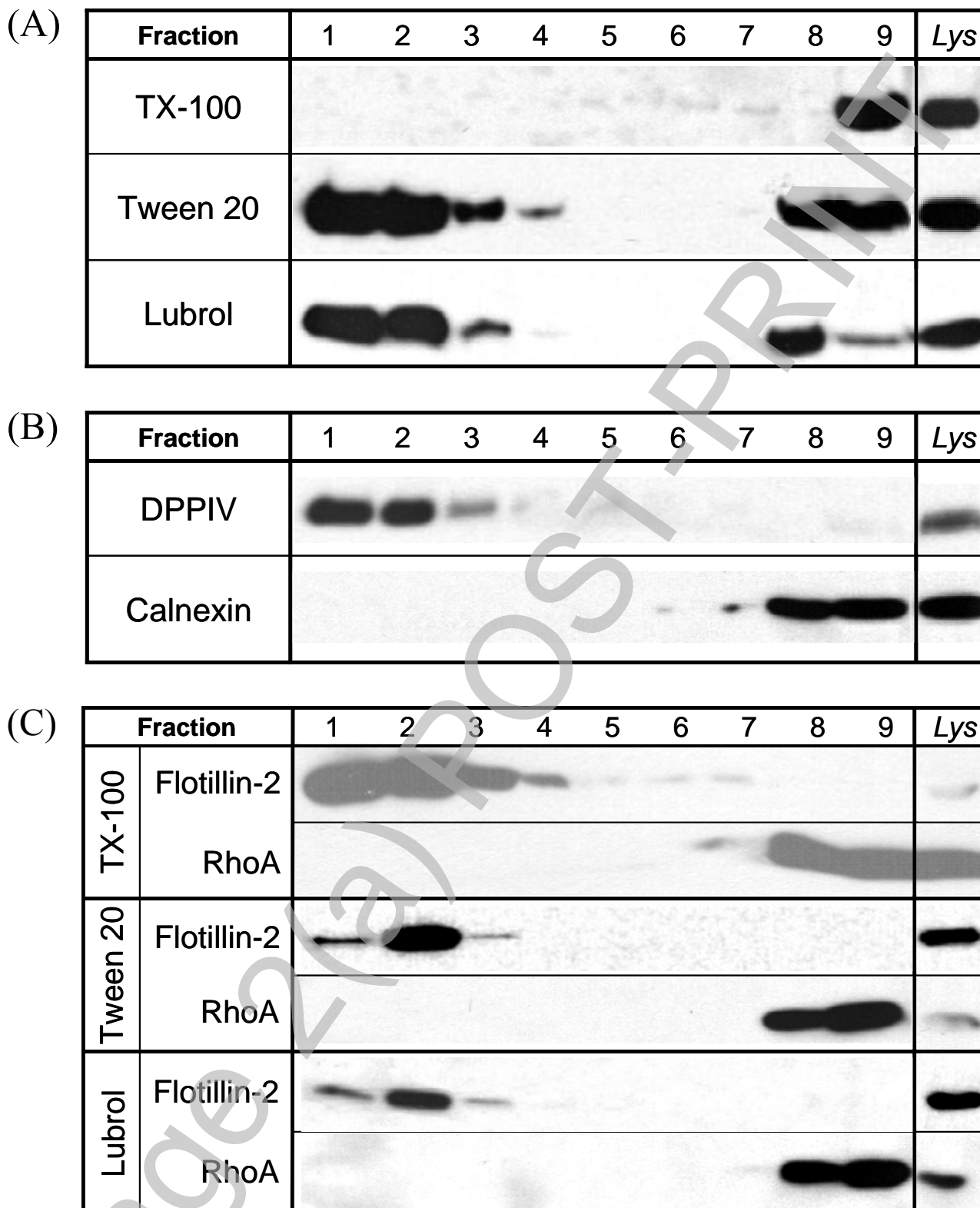
Castelletti et al., Figure 1

THIS IS NOT THE FINAL VERSION - see doi:10.1042/BJ20070396



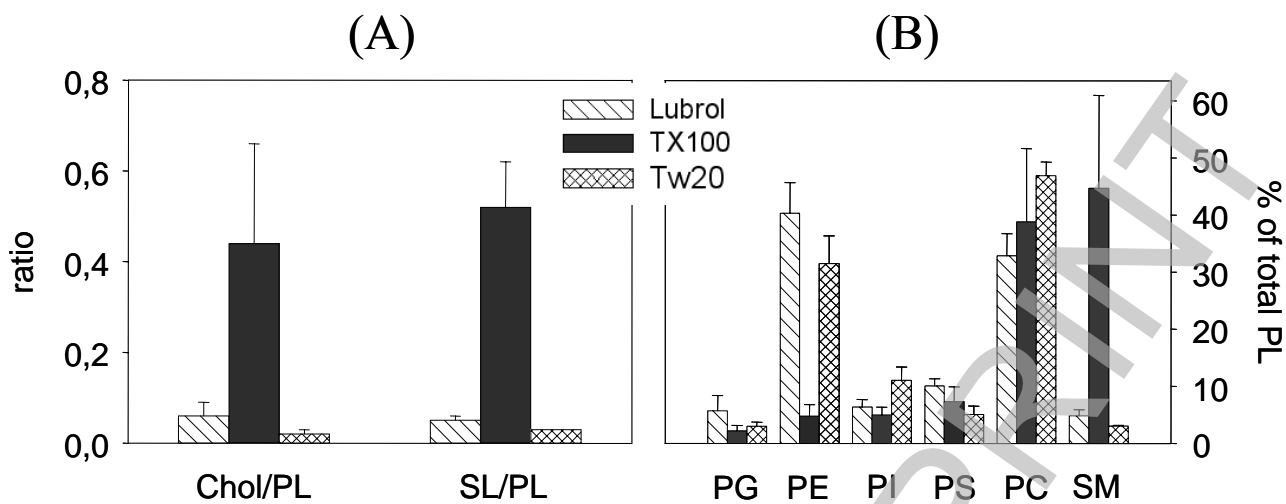
Castelletti et al., Figure 2

THIS IS NOT THE FINAL VERSION - see doi:10.1042/BJ20070396



THIS IS NOT THE FINAL VERSION - see doi:10.1042/BJ20070396

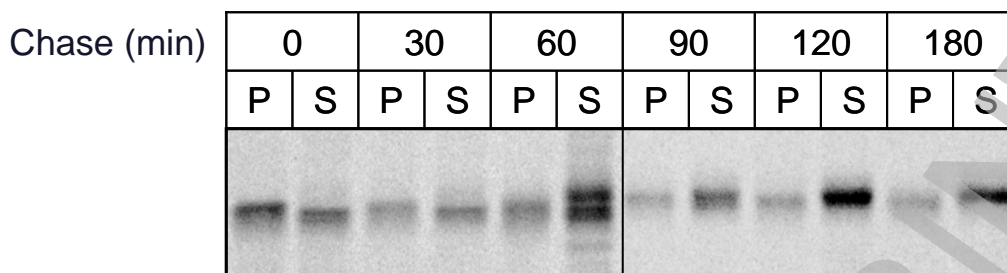
Castelletti et al., Figure 3



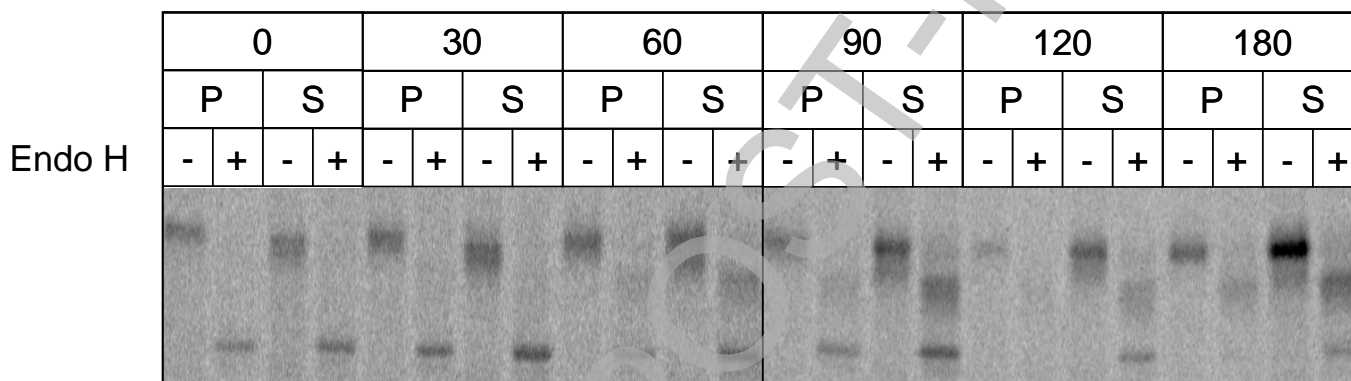
THIS IS NOT THE FINAL VERSION - see doi:10.1042/BJ20070396

Castelletti et al., Figure 4

(A)



(B)

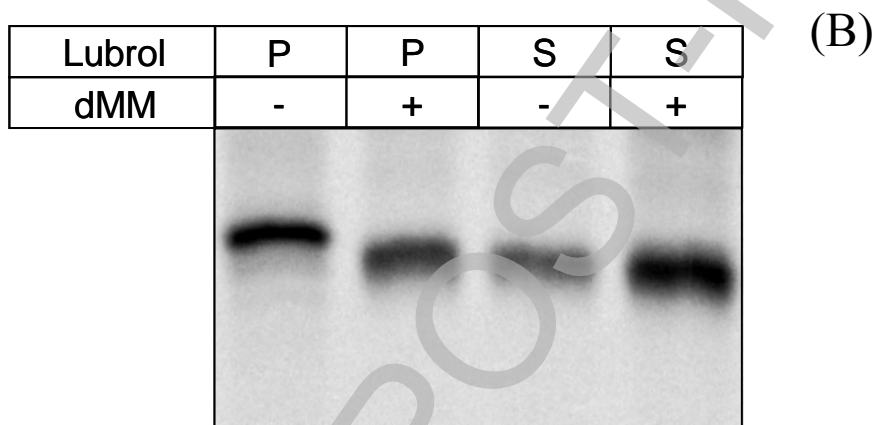
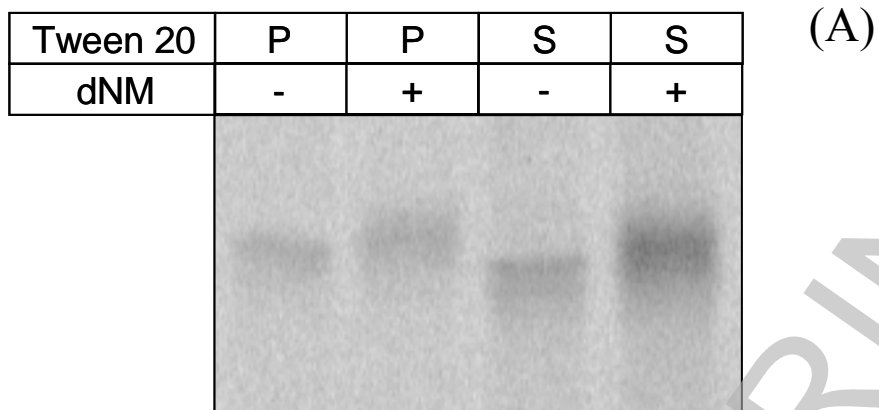


(C)



THIS IS NOT THE FINAL VERSION - see doi:10.1042/BJ20070396

Castelletti et al., Figure 5

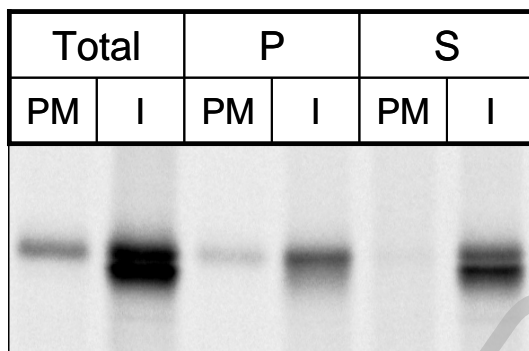


Stage 2(a) POST-PRINT

Castelletti et al., Figure 6

THIS IS NOT THE FINAL VERSION - see doi:10.1042/BJ20070396

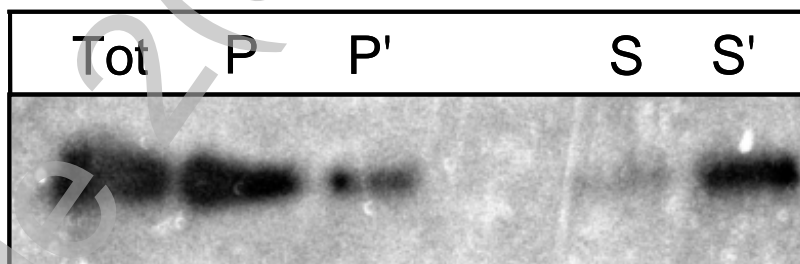
(A)



(B)

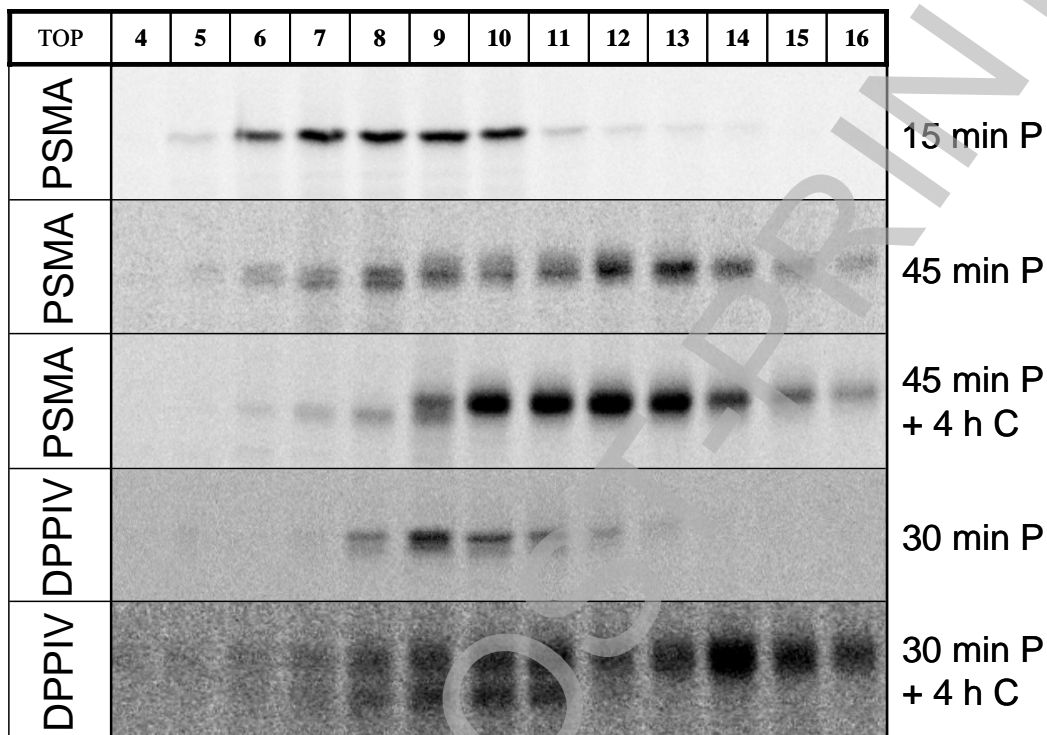


(C)



Castelletti et al., Figure 7

THIS IS NOT THE FINAL VERSION - see doi:10.1042/BJ20070396



THIS IS NOT THE FINAL VERSION - see doi:10.1042/BJ20070396

Stage 2(a) P

Castelletti et al., Figure 8